Bull Tokyo Dent Coll (2020) 61(1): 9–19

Original Article

doi:10.2209/tdcpublication.2019-0008

Temporomandibular Joint Hypofunction Secondary to Unilateral Partial Discectomy Attenuates Degeneration in Murine Mandibular Condylar Cartilage

Mamoru Yotsuya[1,2], **Jose Iriarte-Diaz**[3] **and David A. Reed**[1]

[1] *Department of Oral Biology, College of Dentistry, University of Illinois at Chicago, 801 South Paulina Street, Chicago, IL, United States*
[2] *Department of Fixed Prosthodontics, Tokyo Dental College, 2-9-18 Kanda-Misakicho, Chiyoda-ku, Tokyo 101-0061, Japan*
[3] *Department of Biology, The University of the South, 735 University Ave, Sewanee, TN 37383, United States*

Received 30 January, 2019/Accepted for Publication 21 February, 2019
Published Online in J-STAGE 27 February, 2020

Abstract

Mechanical overloading of the temporomandibular joint (TMJ) promotes both the initiation and progression of TMJ osteoarthritis (OA). New preclinical animal models are needed for the evaluation of the molecular basis of cellular load transmission. This would allow a better understanding of the underlying mechanisms of TMJ-OA pain and disability, and help identify new therapeutics for its early diagnosis and management. The purpose of this study was to evaluate the role of mechanical loading in the progression of TMJ-OA in surgical instability arising from unilateral partial discectomy (UPD) in a murine model. In the theoretical modelling employed, lower joint reaction forces were observed on the chewing (working) side of the TMJ in the murine craniomandibular musculoskeletal system. Hypofunction was induced secondary to UPD through surgically manipulating the working side using an unopposed molar model. When the working side was restricted to the same side as that on which UPD was performed, late-stage degeneration of the cartilage showed a significant reduction ($p<0.05$), with diminished fibrillation and erosion of the articular cartilage, cell clustering, and hypocellularity. Condylar remodelling and proteolysis of proteoglycans were less affected. Thus, select and specific late-stage changes in TMJ-OA were contextually linked with the local mechanical environment of the joint. These data underscore the value of the UPD mouse model in studying mechanobiological pathways activated during TMJ-OA, and suggest that therapeutically targeting mechanobiological stimuli is an effective strategy in improving long-term biological, clinical, and patient-based outcomes.

Key words: Temporomandibular joint — Mandibular condylar cartilage — Hypofunction — Osteoarthritis — Free-body analysis

Introduction

Temporomandibular joint (TMJ) osteoarthritis (OA) is associated with dysfunctional remodelling of the mandibular condylar cartilage, arthralgia, limited joint mobility, and diminished quality of life[20]. The etiopathophysiology of TMJ-OA is ill-defined, and contemporary molecular targets for clinical intervention have yet to be identified. Although systemic illness, aging, and hormonal and behavioral factors have been implicated, growing evidence suggests that mechanical overloading of the articular fibrocartilage is a key factor in the initiation and progression of TMJ-OA[10,12,20,21].

Formative preclinical evaluation of novel therapeutics necessitates the utilization of preclinical animal models that encompass the unique mechanical and metabolic considerations of TMJ-OA[1,2,5]. The surgical instability, unilateral partial discectomy (UPD) murine model produces degenerative changes in the mandibular condylar cartilage that closely match their clinical presentation in humans[17,24,25]. A UPD presents with condylar flattening, osteophyte formation, lipping, sclerosis, proteolysis of proteoglycans, fibrillation, and erosion. Because it is surgically induced, a UPD is post-traumatic. It reproducibly and reliably generates changes in tissue appropriate to TMJ-OA that are ideal for identifying select and specific mechanisms of degeneration of cartilage. It is less clear, however, as to whether the UPD model is also useful in the study of the etiopathophysiology of TMJ-OA. While the UPD procedure destabilizes the TMJ, the role of mechanical loading in the observed degenerative changes has yet to be systematically addressed. The use of a hypofunction model secondary to the UPD procedure would permit the effects of mechanical overloading to be studied in parallel with those from the UPD procedure.

Hypofunction in the TMJ can be achieved in a variety of ways, including appliance therapy[13,14], muscle immobilization[3], and surgical approaches[16]. In the present study, however, a new approach will be evaluated: the unopposed molar model (UM). The UM model has been widely used in orthodontic studies of tooth eruption[15,22], but has limited use in the study of the TMJ. In this procedure, the maxillary molars and mandibular incisor are removed unilaterally, constraining the chewing side contralateral to the UM procedure. Theoretical work in non-murine model systems has demonstrated that the TMJ on the chewing side (referred to as the working side, hereafter) is subject to lower joint reaction forces than that on the non-chewing side (the balancing side, hereafter)[4,6,18]. The working and balancing side joint reaction forces in a murine model under different chewing conditions are not known.

The goals of this study were to 1) determine if surgically constraining the working side in a murine model lowered the joint reaction forces to which it was subjected; and 2) evaluate the efficacy of the UM murine model in experimentally inducing hypofunction in a UPD joint and attenuating the progression of degeneration in the TMJ cartilage.

Materials and Methods

1. Calculation of joint reaction forces in murine model during unilateral biting

Murine bite and joint reaction forces were calculated from equations derived from a 3-dimensional (3D), free-body analysis of the orofacial musculoskeletal system[18]. These equations require estimates of the location, direction, and magnitude of jaw adductor muscle forces, and the location of the bite point. To estimate the location, direction, and magnitude of the jaw adductor muscle forces on the murine mandible and skull, muscle attachment areas were digitized from micro-CT scans of *mus musculus* obtained from Digimorph[19]. Virtual muscle segments connecting the cranium and mandible were rendered from these attachment areas and exported as a 3D model[11]. The anterior- and posterior-most elements were identified and used to define 10 equidistant, connected points on each 3D surface. The 10 points representing

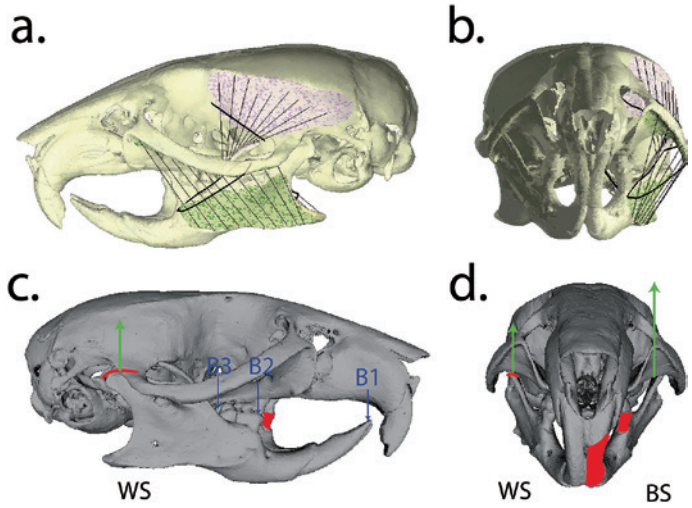

Fig. 1 Joint reaction force calculations

Illustration of jaw adductor sectional area calculated from 3D osteological correlates (a–b) and diagram of surgical procedures/experimental design. Medial (a) and frontal (b) views of temporalis (pink) and masseter (yellow) mapped on μCT scan of mouse skull with maximum cross-sectional area mapped on volume. These cross-sectional area values were used to estimate muscle force and calculate joint reaction forces in free-body analysis. Bite points for free-body analysis were chosen based on positions calculated from μCT scan. The unilateral partial discectomy (UPD) procedure was always performed on right side and unopposed molar (UM) procedure always on left side, forcing chewing to occur ipsilateral to the UPD (c–d). The chewing side is working side (WS) and non-chewing side balancing side (BS).

the cranial segment were then connected with the 10 points representing the mandibular segment. These connected segments were used to define the direction of the muscle line of action (thin black lines on Figs. 1a and 1b).

In this free-body analysis, absolute forces are not necessary to calculate working and balancing side joint reaction force ratios. Therefore, the model assumptions permit muscle forces equal to cross-sectional area rather than absolute muscle values. The cross-sectional area was calculated using a 3D convex hull approach (*i.e.*, the smallest convex polygon), with the cross-sectional area of the muscle (A_{cs}) defined as the largest cross-sectional area of the convex hull normal to the line connecting the centroid of the cranium muscle attachment and the centroid of the mandible cranium attachment (thick black lines in Figs. 1a and 1b). Muscle forces were defined in arbitrary units squared (au^2), with masseter equal to 4.82 au^2, medial pterygoid equal to 4.37 au^2, and temporalis equal to 3.13 au^2.

These estimated, relative muscle forces were then entered into the equations derived from free-body analysis to calculate bite force and working/balancing side joint reaction forces. The methods employed were based on those of Reed, Iriarte-Diaz *et al*[18]. In brief, the equations must assume that the system of forces is in static equilibrium, with the sum of all forces and moments equal to zero. Bite force (F_{BP}) is calculated according to the following equation:

$$F_{BP} = \frac{-\sum\left(p_{Mz}F_{Mx} - p_{Mx}F_{Mz}\right)}{p_{BPx}}$$

where p_{Mx} and p_{Mz} are the X (antero-posterior) and Z (dorso-ventral) positions of the muscle

attachment at the mandible with respect to the origin; F_{Mx} and F_{Mz} are the Y and Z components of the muscle forces; and p_{BPx} is the X-position of the bite point.

The joint reaction forces for the working (F_{Jws}) and balancing sides (F_{Jbs}) are calculated according to the following equations:

$$F_{Jws} = \sqrt{\left(-\frac{F_{MTx}}{2}\right)^2 + \left[\left(-\frac{F_{MTz}}{2}\right) - \frac{F_{BP}}{2}\left(1 + \frac{p_{BPy}}{p_{Jy}}\right)\right]^2}$$

$$F_{Jbs} = \sqrt{\left(-\frac{F_{MTx}}{2}\right)^2 + \left[\left(-\frac{F_{MTz}}{2}\right) - \frac{F_{BP}}{2}\left(1 - \frac{p_{BPy}}{p_{Jy}}\right)\right]^2}$$

where F_{MTx} and F_{MTz} are the X and Z components of the sum of all muscle forces; and p_{BPy} and p_{Jy} are the y-position (antero-posterior) of the bite point and the jaw joint. The working/balancing side ratio is calculated, with a ratio approaching 1 indicating equal loading at the joints, and a ratio of <1 indicating greater loading on the balancing side. Previous analyses have illustrated that a ratio of >1 is not permitted under normal physiological loading in equilibrium[18].

2. Unilateral partial discectomy model

Temporomandibular joint osteoarthritis was induced by unilateral partial discectomy[24,26]. Seven-week-old, male c57 BL/6J mice were anesthetized with ketamine (100 mg/kg) and xylazine (5 mg/kg). The lateral capsule was exposed and incised, taking a posterior approach on the right joint (Fig. 1). The articular disc was excised, the joint irrigated with sterile saline, and the wound closed with 5-0 Ethilon sutures. Sham control surgeries were identical, except the lateral capsule and disc were left intact. Experimental endpoints included 4 time points: 4, 8, 12, and 16 weeks postoperatively. These time points were chosen based on previous descriptions of the mouse model[24]. No special diet was necessary postoperatively, and no adverse health effects were observed. All experiments using vertebrate animals were approved by the University of Illinois at Chicago Animal Care Committee and performed in accordance with the relevant guidelines and regulations.

Table 1 Modified Mankin score definition table

Pericellular safranin-O staining	
Normal	0
Slightly enhanced	1
Intensely enhanced	2
Background safranin-O staining	
Normal	0
Slight increase or decrease	1
Severe increase or decrease	2
No staining	3
Arrangement of chondrocytes	
Normal	0
Apprearance of clustering	1
Hypocellularity	2
Cartilage structure	
Normal	0
Fibrillation in superficial layer	1
Fibrillation beyond superficial layer	2
Missing articular cartilages	3

Table defining Modified Mankin scoring following Xu *et al.* (2009)

3. Unilateral unopposed molar model

The working side was controlled surgically by unilateral extraction of the maxillary molars and clipping of the mandibular incisor contralateral to the UPD (left side). Therefore, postoperative mastication occurs ipsilateral to the affected TMJ (right side; Fig. 1). The molars were extracted immediately following the UPD procedure. A dental scaler was placed on the posterior crown and pressure applied until the tooth was extracted. The socket was then irrigated with sterile saline and pressure applied until bleeding stopped. The mandibular incisor contralateral to the UPD was clipped every 2 weeks for the duration of the experiment to prevent the still-growing teeth from coming into occlusion.

4. Histology and grading of cartilage degeneration

Tissue samples were fixed in 4% PFA for

Table 2 Joint reaction force calculations

Bite Position	Molar_Distal	Molar_center	Molar_Mesial	Diastema	Incisor
Bite Force (R, UPD side)	−71.98	−63.94	−55.33	−48.79	−25.29
Reaction Force (L, BS, UM side)	95.56	98.99	101.14	102.35	103.37
Reaction force (R, WS, UPD side)	63.16	67.76	74.23	79.56	102.04
Ratio	0.66	0.68	0.73	0.78	0.99

Values from free-body analysis demonstrating how changes in bite point altered bite force, balancing side joint reaction force (contralateral to UPD), working side joint reaction force (ipsilateral to UPD), and ratio of working to balancing side reaction forces.

18–24 hr, decalcified with 4.5% EDTA for 28 days, and paraffin embedded. Tissue blocks were serially sectioned in the frontal plane at a thickness of 8 μm. For the histomorphometric analysis, all the sections to be analyed were deparaffinized and the nuclei stained with Weigert's iron hematoxylin for 10 min, fast green for 15 min, and safranin O for 15 min. The stained sections were then imaged on a Leica DM 2000 LED microscope using a 20x objective. The progression of TMJ-OA at each time point was quantified using the Modified Mankin Score (Table 1). Modified Mankin scores were statistically compared using a one-way ANOVA.

Results

1. Unopposed molar model lowers joint reactions forces ipsilateral to surgical side

Five bite positions were used in the calculation. In all cases, the working side joint reaction forces were lower than those on the balancing side in mouse, with the difference increasing at more distal bite points. The highest bite force was found at the distal-most molar and the lowest at the incisor. Following the predictions of previous work in other animal models, unilateral biting yielded higher joint reaction forces on the balancing side than on the working side. Joint reaction forces were highest during incisor biting and lowest during biting on the distal molar. The largest difference between the working and balancing side joint reactions forces occurred during chewing on the distal-most molar. These data revealed that restricting the biting position to one side of the mandible lowered joint reaction forces on the working side (Table 2).

2. Hypofunction secondary to unilateral partial discectomy attenuates cartilage degeneration

In both the UPD-only and UM + UPD models, there was evidence of degeneration at all time points on the right side (the side of the UPD procedure). At 4 weeks postoperatively, there was condylar remodelling and a slight increase in background proteoglycan. Differences between the two experimental groups became clear at 8 weeks postoperatively, with fibrillation in the articular cartilage of the UPD-only model and no apparent change in the articular cartilage in the UM + UPD model. However, a slight decrease was observed in overall background proteoglycan in the UM + UPD model. This difference was accentuated at 12 weeks. In the UPD-only model, fibrillations extended beyond the superficial layer, with proteolysis of proteoglycans and cell clustering. The 12-week UM + UPD tissue showed no difference to that at 8 weeks. At 16 weeks postoperatively, elevated levels of hypocellularity and erosion of the articular cartilage were observed in the UPD-only model. In the UM + UPD model, slight fibrillation was apparent in the articular cartilage at this stage, but the cell morphology, cell number, and cartilage integrity appeared unchanged (Fig. 2).

Similar degenerative changes occurred on

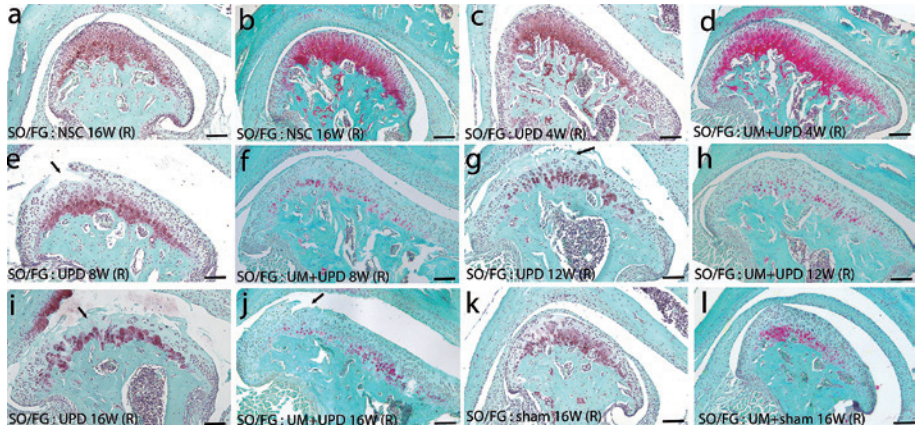

Fig. 2 Cartilage degeneration in UM + UPD and UPD murine models

Representative safranin-o/fast green stained (SO/FG) sections from UM + UPD and UPD-only experimental groups demonstrating differences in cartilage degeneration in mandibular condyles in joints in non-surgical (a–b), 4-week (c–d), 8-week (e–f), 12 week (g–h), 16 week (i–j), and 16 weeks sham control (k–l) groups. All scale bars equal 50 μm.

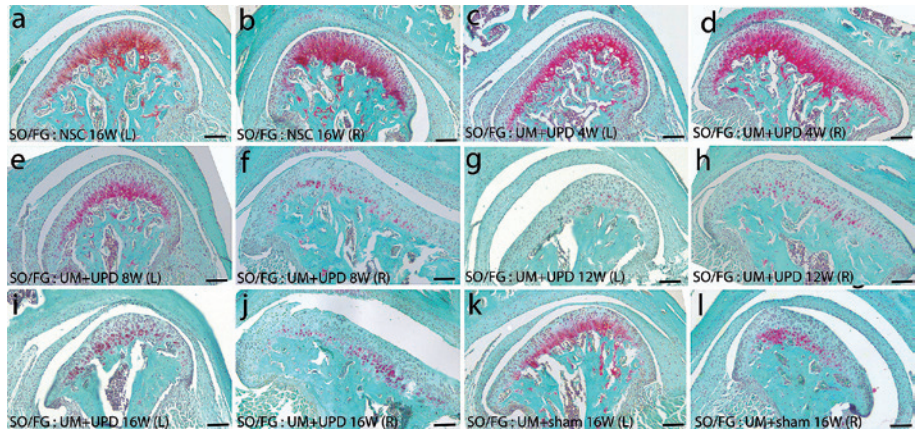

Fig. 3 Cartilage degeneration in UM + UPD murine model

Representative safranin-o/fast green (SO/FG) stained sections from UM + UPD experimental group demonstrating differences in cartilage degeneration in mandibular condyles ipsilateral (R) and contralateral (L) to UPD in non-surgical control (a–b), 4 week (c–d), 8 week (e–f), 12 week (g–h), 16 week (i–j), and 16 weeks sham control (k–l) groups. All scale bars equal 50 μm.

the left joint (the side of the UM procedure). The left joint was the balancing side joint. According to free-body analysis, the joint reactions forces were elevated on this side at all bite points. The left joint appeared unaffected by the UM + UPD procedure until approximately 12–16 week postoperatively. At this experimental stage, background safranin-o staining showed a decrease, and there was an increase in pericellular safranin-o staining (Fig. 3). Similar changes were observed in the left joint of the UPD only tissues.

A statistical comparison revealed that the rate of increase in the Modified Mankin

Scores was greater on the right side in the UPD-only model than that in the UM + UPD model. This yielded significantly lower stages of degeneration in the UM + UPD model at 8, 12, and 16 weeks postoperatively. No significant difference was observed between the UPD-only and the UM + UPD models on the left side, however. Therefore, the observed increase in degenerative change contralateral to the UPD was consistent with the UPD, not the UM procedure (Fig. 4, Table 3, 4).

Although a comparison between sides in the UM + UPD model revealed significant differences at 4–8 weeks postoperatively, no such difference was observed at 12–16 weeks, indicating that the rate of degenerative change within the right-side joint approaches that of the unaffected side when joint reaction forces are mitigated through surgical control of the bite side (Fig. 4, Table 5).

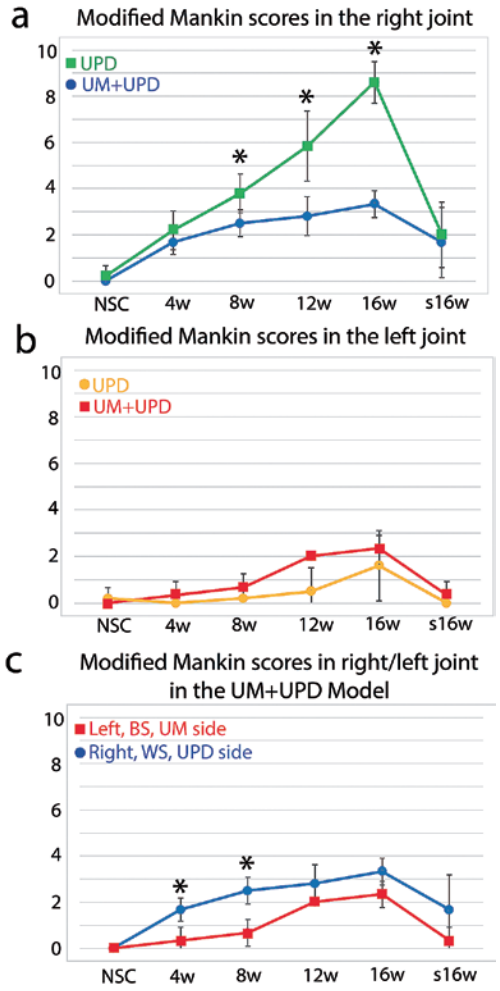

Fig. 4 Modified Mankin scores

Graphs of average Modified Mankin scores at each time point in UPD-only and UM + UPD experimental groups comparing right, WS, UPD side joint (a) left, BS, UM side joint (b), and right/left in UM + UPD model (c). Modified Mankin score of 10 indicates high degree of degeneration and score of 0 indicates normal joint. Asterisks denote significant differences as indicated in Tables 3–5. Experimental groups are defined as non-surgical control (NSC), 4-week (4w), 8-week (8w), 12-week (12w), 16-week (16w), and 16-week sham control (s16w).

Discussion

The results of the present study using a theoretical, free-body approach revealed that unilateral biting in a murine musculoskeletal system lowered the working-side joint reaction forces at all positions on the tooth row. Furthermore, empirical murine model data showed that surgically restricting the bite side using the UM model to the side of the UPD attenuated the progression of degeneration in mandibular condylar cartilage. As a surgical instability model, the UPD approach is post-traumatic, so etiopathophysiology could be multifactorial. Taken together, the present theoretical and empirical data support the hypothesis that mechanical loading secondary to UPD is a critical determinate of cartilage degeneration in this murine model, and underscore the key role of mechanobiological signalling pathways in the etiopathophysiology of TMJ-OA.

Precisely defining the mechanical microenvironment associated with TMJ-OA is an important next step, and will require more complex theoretical models. The free-body approach is limited because it assumes that the mandible is a rigid body. In contrast to in humans, the mouse jaw is comprised of two hemimandibles joined together by an unfused symphysis. The unfused symphysis is hypothesized to be ineffective for the transfer of bal-

Table 3 Comparison of Modified Mankin scores in UPD-only and UM + UPD model on right side

Right, WS, UPD side	NSC	4w	8w	12w	16w	s16w
UPD only model						
Mean	0.20	2.20	3.80	5.83	8.60	2.00
SD	0.45	0.84	0.84	1.52	0.89	1.41
UPD + UM model	0.00	0.00	0.00	0.00	0.00	0.00
Mean	0.00	1.67	2.50	2.80	3.33	1.67
SD	0.00	0.52	0.58	0.84	0.58	1.53
ANOVA	$F(1,7)=0.78$, $p=0.41$	$F(1,9)=1.69$, $p=0.23$	$F(1,7)=6.92$, $p<0.05$	$F(1,9)=16.57$, $p<0.05$	$F(1,6)=80.70$, $p<0.05$	$F(1,6)=0.10$, $p=0.76$

Comparison of average value, standard deviation, and ANOVA in Modified Mankin scores at each time point between UPD-only and UM + UPD models on right joint (working side, ipsilateral to UPD procedure). Experimental groups are defined as non-surgical control (NSC), 4-week (4w), 8-week (8w), 12-week (12w), 16-week (16w), and 16-week sham control (s16w).

Table 4 Comparison of Modified Mankin scores in UPD-only and UM + UPD model on left side

Left, BS, UM side	NSC	4w	8w	12w	16w	s16w
UPD only model						
Mean	0.20	0.00	0.20	0.50	1.60	0.00
SD	0.45	0.00	0.45	1.00	1.52	0.00
UPD + UM model						
Mean	0.00	0.33	0.67	2.00	2.33	0.33
SD	0.00	0.58	0.58	0.00	0.58	0.58
ANOVA	$F(1,7)=0.78$, $p=0.41$	$F(1,4)=1.00$, $p=0.38$	$F(1,7)=1.67$, $p=0.24$	$F(1,5)=6.43$, $p=0.052$	$F(1,6)=0.61$, $p=0.46$	$F(1,6)=1.88$, $p=0.22$

Comparison of average value, standard deviation, and ANOVA in Modified Mankin scores at each time point between UPD only and UM + UPD models on left joint (non-chewing side, contralateral to UPD procedure). Experimental groups are defined as non-surgical control (NSC), 4-week (4w), 8-week (8w), 12-week (12w), 16-week (16w), and 16-week sham control (s16w).

ancing-side jaw adductor muscle forces to the bite point[7–9]. A second biological factor, which was not incorporated into our model, was that mice primarily ingest their food using the incisors. Even unilateral incision yields a working-side joint reaction force nearly equal to that on the balancing side (Table 1). Furthermore, mice can bilaterally reduce food on the molars due to a propalinal (anteroposterior) jaw shift[23], requiring complex translational movements of the TMJ. The free-body approach used in the present study assumes a rigid body in equilibrium, and cannot resolve tractional/translational forces on the articu-

Table 5 Comparison of Modified Mankin scores of right and left joint in UM + UPD model

UM + UPD Right/Left	NSC	4w	8w	12w	16w	s16w
Right, WS, UPD side						
Mean	0.00	1.67	2.50	2.80	3.33	1.67
SD	0.00	0.50	0.58	0.82	0.58	1.53
Left, BS, UM side						
Mean	0.00	0.33	0.67	2.00	2.33	0.33
SD	0.00	0.58	0.58	0.00	0.58	0.58
ANOVA	$F(1,6) = na$, $p = 0$	$F(1,7) = 12.44$, $p < 0.05$	$F(1,5) = 17.28$, $p < 0.05$	$F(1,6) = 2.57$, $p = 0.16$	$F(1,4) = 4.5$, $p = 0.10$	$F(1,4) = 2.0$, $p = 0.23$

Comparison of average value, standard deviation, and ANOVA in Modified Mankin scores at each time point between right and left joint in UM + UPD model.
Experimental groups are defined as non-surgical control (NSC), 4-week (4w), 8-week (8w), 12-week (12w), 16-week (16w), and 16-week sham control (s16w).

lar surface of the condyle. The relative impact of translational versus compressive forces on cartilage tribology is an important next step that will require more complex modelling.

Despite the drawbacks inherent to the assumptions of the model used here, however, the empirical data unequivocally demonstrated that the UM + UPD approach attenuated the progression of degeneration in the mandibular condylar cartilage when compared to that seen in the UPD-only model. Since UM alone had no impact on the Mankin Score after 16 weeks, and the UM surgical site was not anatomically related the UPD surgical site, these data point to an initiating factor localized to the joint space. As such, the fibrillation, erosion, cell clustering, and hypocellularity associated with the advanced TMJ-OA observed in the UPD model can be at least contextually linked with the local mechanical environment of the articular cartilage predicted from our theoretical model.

Perhaps equally as intriguing are the characteristics associated with the TMJ-OA-affected joint that were not impacted by the UM procedure. Hypofunction did not impact the immediate remodelling of the bony condyle or the long-term degradation of safranin-o stained proteoglycans. In fact, lower safranin-o staining was observed in the sham controls and on the left (UM side) mandibular condyle.

Together, these data demonstrate that there are select and specific late-stage changes in TMJ-OA contextually linked with mechanically activated signalling pathways. Furthermore, these data underscore the value of the UPD mouse model in the study of mechanobiological pathways activated during post-traumatic TMJ-OA, and suggest that therapeutically targeting mechanobiological stimuli is an effective strategy in improving long-term biological, clinical, and patient-based outcomes.

Acknowledgements

This work was supported by the UIC Department of Oral Biology. Research reported in this publication was also supported by the National Center for Advancing Translational Sciences of the National Institutes of Health under Award Number 5R03DE026248-02 and 3KL2TR002002-02S1. The content is solely the responsibility of the authors and does not

necessarily represent the official views of the National Institutes of Health. The authors declare no potential conflict of interest with respect to the authorship and/or publication of this article. DR conceived the experiments; MY, JI, and DR conducted the experiments. All authors analyzed and interpreted the results; all authors were involved in the drafting and critical review of the manuscript. The authors declare no competing financial interests. All relevant data are within the paper.

References

1) Almarza AJ, Brown BN, Arzi B, Ângelo DF, Chung W, Badylak SF, Detamore M (2018) Preclinical animal models for temporomandibular joint tissue engineering. Tissue Engineering Part B: Reviews 24:171–178.
2) Almarza AJ, Hagandora CK, Henderson SE (2011) Animal models of temporomandibular joint disorders: Implications for tissue engineering approaches. Ann Biomed Eng 39: 2479–2490.
3) Dutra EH, O'brien MH, Logan C, Tadinada A, Nanda R, Yadav S (2018) Loading of the condylar cartilage can rescue the effects of botox on tmj. Calcif Tissue Int 103:1–9.
4) Greaves WS (1982) A mechanical limitation on the position of the jaw muscles of mammals: The one-third rule. J Mammal 63: 261–266.
5) Herring SW (2003) Tmj anatomy and animal models. J Musculoskelet Neuronal Interact 3: 391–394; discussion 406–407.
6) Hylander WL (1985) Mandibular function and biomechanical stress and scaling. American Zoology 25:315–330.
7) Hylander WL (1984) Stress and strain in the mandibular symphysis of primates: A test of competing hypotheses. Am J Phys Anthropol 64:1–46.
8) Hylander WL, Ravosa MJ, Ross CF, Johnson KR (1998) Mandibular corpus strain in primates: Further evidence for a functional link between symphyseal fusion and jaw—adductor muscle force. American Journal of Physical Anthropology: The Official Publication of the American Association of Physical Anthropologists 107:257–271.
9) Hylander WL, Ravosa MJ, Ross CF, Wall CE, Johnson KR (2000) Symphyseal fusion and jaw-adductor muscle force: An emg study. Am J Phys Anthropol 112:469–492.
10) Ikeda Y, Yonemitsu I, Takei M, Shibata S, Ono T (2014) Mechanical loading leads to osteoarthritis-like changes in the hypofunctional temporomandibular joint in rats. Arch Oral Biol 59:1368–1376.
11) Iriarte-Diaz J, Terhune CE, Taylor AB, Ross CF (2017) Functional correlates of the position of the axis of rotation of the mandible during chewing in non-human primates. Zoology 124:106–118.
12) Kaul R, O'brien MH, Dutra E, Lima A, Utreja A, Yadav S (2016) The effect of altered loading on mandibular condylar cartilage. PLoS ONE 11: e0160121.
13) Kunii R, Yamaguchi M, Aoki Y, Watanabe A, Kasai K (2007) Effects of experimental occlusal hypofunction, and its recovery, on mandibular bone mineral density in rats. The European Journal of Orthodontics 30:52–56.
14) Liu J, Jin Z-L, Li Q (2015) Effect of occlusal hypofunction and its recovery on the three-dimensional architecture of mandibular alveolar bone in growing rats. J Surg Res 193: 229–236.
15) Luan X, Diekwisch TG (2007) Vienna-chicago: The cultural transformation of the model system of the un-opposed molar. Bioessays 29: 819–830.
16) Miyazaki M, Yonemitsu I, Takei M, Kure-Hattori I, Ono T (2016) The imbalance of masticatory muscle activity affects the asymmetric growth of condylar cartilage and subchondral bone in rats. Arch Oral Biol 63: 22–31.
17) Polur I, Lee PL, Servais JM, Xu L, Li Y (2010) Role of htra1, a serine protease, in the progression of articular cartilage degeneration. Histol Histopathol 25:599–608.
18) Reed DA, Iriarte-Diaz J, Diekwisch T (2016) A three dimensional free-body analysis describing variation in the musculoskeletal configuration of the cynodont lower jaw. Evol Dev 18: 41–53.
19) Rowe T (2002) Digimorph: A national science foundation digital library at the university of texas at austin. Http. digimorph. org.
20) Tanaka E, Detamore M, Mercuri L (2008) Degenerative disorders of the temporomandibular joint: Etiology, diagnosis, and treatment. J Dent Res 87:296–307.
21) Utreja A, Dyment NA, Yadav S, Villa MM, Li Y, Jiang X, Nanda R, Rowe DW (2016) Cell and matrix response of temporomandibular cartilage to mechanical loading. Osteoarthritis Cartilage 24:335–344.
22) Walker CG, Ito Y, Dangaria S, Luan X, Diekwisch TG (2008) Rankl, osteopontin, and

osteoclast homeostasis in a hyperocclusion mouse model. Eur J Oral Sci 116:312–318.
23) Weijs W (1975) Mandibular movements of the albino rat during feeding. J Morphol 145: 107–124.
24) Xu L, Polur I, Lim C, Servais J, Dobeck J, Li Y, Olsen B (2009) Early-onset osteoarthritis of mouse temporomandibular joint induced by partial discectomy. Osteoarthritis Cartilage 17: 917–922.
25) Xu L, Servais J, Polur I, Kim D, Lee PL, Chung K, Li Y (2010) Attenuation of osteoarthritis progression by reduction of discoidin domain receptor 2 in mice. Arthritis Rheum 62: 2736–2744.
26) Yotsuya M, Bertagna AE, Hasan N, Bicknell S, Sato T, Reed DA (2019) Neuron/glial antigen 2-type vi collagen interactions during murine temporomandibular joint osteoarthritis. Scientific Reports 9:56.

Correspondence:
David A. Reed
Department of Oral Biology,
College of Dentistry,
University of Illinois at Chicago,
801 South Paulina, Chicago, IL,
United States
E-mail: reedd@uic.edu